Journal of Engineering Physics and Thermophysics, Vol. 83, No. 6, 2010

PANORAMIC DIAGNOSTICS OF SURFACE TEMPERATURES AND HEAT FLUXES IN AN AERODYNAMIC EXPERIMENT

G. M. Zharkova and V. N. Kovrizhina UDC 532.783

The principles of visualization and measurement of surface temperatures and heat fluxes by the method of liquid-crystal tomography in an aerophysical experiment are described. The properties of polymeric liquid-crystal, heat-sensitive coatings and application of them in subsonic and hypersonic facilities for investigating the structure of a near-wall flow and aerodynamic heating are considered.

Keywords*: liquid crystals, cholesteric liquid crystals, polymeric liquid-crystal, heat-sensitive coatings, liquid-crystal tomography.*

Introduction. The optical methods of visualization and temperature measurement on a solid surface blown by a gas flow which are based on the change in the optical properties of thin-film coatings have attracted the attention of researchers by their simplicity and by the possibility of obtaining a panoramic picture of a temperature field. It is known that any disturbance of a flow is accompanied by a change of temperature in a boundary layer. Therefore, visualization and measurement of the distribution of temperature near a blown surface allow one to identify such structural characteristic features of a flow as transition of a laminar flow into a turbulent one, separation and reattachment of flow, influence of shock waves on a boundary layer, etc. Film coatings altering their optical properties under the action of a gas flow make it possible to register temperature distribution over a large area at one instant of time. To the obvious advantages of these methods one should assign the relative simplicity of preparation of the model surface, not requiring rather complex piercing of the model for installing various types of probes. Application of film coatings opens up the way for increasing the informativeness and making an experiment much cheaper.

To date, a common instrument for panoramic visualization and measurement of temperature fields on a surface in an aerophysical experiment are thin-film coatings based on liquid crystals sensitive to temperature [1–3]. This has become possible due to the introduction of automated digital processing of color images with a high spatial and temporal resolution and creation of software for secondary processing of information.

Liquid-crystal thermography (LCT) has long been applied for visualizing and measuring temperature fields and heat fluxes in an aerodynamic experiment [1–4]. The refinement of the method was due to new developments of liquid-crystal materials and creation of respective optical schemes of illumination and registration of a color image and of the algorithms of processing images for obtaining quantitative results. A wealth of experience has been gained on application of thin-film coatings in many scientific and engineering applications in various facilities in Japan, the USA, Russia, Great Britain, and in other European countries. To date, progress in the development of the LCT method in Russia is due to the works carried out at the S. A. Khristianovich Institute of Theoretical and Applied Mechanics of the Siberian Branch of the Russian Academy of Sciences (ITAM): a heat-sensitive material has been created and a method of visualization and measurement of temperature fields and heat fluxes to fit the Institute's facilities has been developed.

The present work gives a brief overview of the results obtained: the properties of the polymeric liquid-crystal films developed at the Institute and the basic principles of application of coatings in aerodynamic experiments at subsonic and hypersonic flow velocities are described.

Polymeric Liquid-Crystal Films. Liquid crystals (LC) constitute a large class of compounds (primarily organic) characterized by orientational order [5–7]. For temperature indication, cholesteric liquid crystals (CLC) charac-

S. A. Khristianovich Institute of Theoretical and Applied Mechanics, Siberian Branch of the Russian Academy of Sciences, 4/1 Institutskaya Str., Novosibirsk, 630090, Russia; email: zharkova@itam.nsc.ru. Translated from Inzhenerno-Fizicheskii Zhurnal, Vol. 83, No.6, pp.1072–1083, November–December, 2010. Original article submitted March 30, 2010.

terized by a periodic helical structure with a certain pitch are used. Such a structure possesses the properties of a uniaxial negative crystal. When an unpolarized white light passes through a thin CLC layer with a planar texture (the helix axis is perpendicular to the surface), it decomposes into two waves with opposite circular polarization. Depending on the CLC structure (the right helix or the left one), one wave passes as it is, whereas the other is reflected selectively. The effect of selective Bragg reflection appears when the incident-light wavelength is close to the pitch of the helix. If the helix's pitch corresponds to the wavelengths of visible range, the surface appears colored. It is this optical effect of liquid crystals — the temperature dependence of the wavelength of selective reflection on temperature — on which the LCT method is based.

Since the structural elements of liquid crystals are bound by rather weak dispersion forces, small external effects (temperature, mechanical shear, electric and magnetic fields) alter the pitch of the helix and respectively the wavelength of the reflected light. The pitch of the helix depends on the chemical structure of the CLC compounds. Therefore, in order that the pitch of the CLC helix correspond to the visible-light wavelengths in the assigned temperature interval, one mixes several compounds with different pitches.

In aerodynamic experiments, an LC coating applied to a surface is subjected to the simultaneous action of temperature and surface friction. To separate the influence of these two factors on the cholesteric helix pitch when they are used to measure temperature, it is necessary to protect the LC from the influence of mechanical shear. Among the means of protection is encapsulation of the LC into a polymeric matrix [8]. The choice of the polymeric matrix and the method of encapsulation is determined by the conditions of the experiment in which they will be used. The material formed by encapsulation of liquid crystals can be obtained either in the form of a film or a dispersion of individual capsules in any isotropic medium.

Heat-sensitive compositions of liquid crystals based on the cholesteryl ester and the technique of their encapsulation into a polymeric matrix have been developed at the ITAM. Temperature-indicating films consist of a lawsone base black in color onto which a temperature-sensitive layer — liquid crystals encapsulated into a polymer — is applied by the method of coating. The thickness of the temperature-sensitive layer must amount to 10–15 μm.

The working range of the temperatures of the film depending on the LC composition may vary from −10 to +200°C, with the threshold sensitivity being equal to $5 \cdot 10^{-4}$ W/cm^2 .

Method of Application of Temperature-Indicating Films. The technique of using polymeric liquid-crystal temperature indicators is described in a number of publications [9–11]. Along with the general principles that should be complied with in using temperature indicators, there exist certain characteristic features in each specific case. First, it is necessary to approximately know the temperature region in which an LC coating will function. Second, a coating must not disturb the thermal field of the test surface, i.e., the heat capacity of the test surface must exceed that of the LC coating. Third, the rate of change of a temperature field must be smaller than the time constant of the CLC coatings used. A temperature-sensitive coating can be formed directly on the test surface by the sputtering technique or by gluing a prepared film to the surface. Usually in subsonic flows the test surface should be heated beforehand. In experiments, the temperature field of the surface cooled by an encircling flow is visualized. In contrast to subsonic flows, in hypersonic facilities the heating of the model surface is registered.

The thus-prepared object of investigation is installed in the test chamber of a wind tunnel and is exposed to white light. The color picture of the temperature field obtained in an experiment is fixed by a video camera.

For quantitative interpretation of the color picture, the temperature-sensitive coating is calibrated. The optical scheme of a calibrating device must be identical to that employed in a real experiment. Thus, the measurement of temperature is reduced to the measurement of color (calorimetry) in a certain system of tristimulus values. The linear system *RGB* applied in color television is the Cartesian coordinate system constructed in conformity with the three-component theory of color vision. Since CLC reflect pure spectral colors, this model is not ideal for exact identification of color. Therefore, for measuring the color of an LC coating, we use the nonlinear *HSI* system in which a color is determined by a hue H, saturation S, and intensity I [10]. On change in temperature, the hue H, in contrast to the coordinates R, G, and B, changes monotonically; therefore the function $H(T)$ can be used for the calibration and measurement of temperature. Typical calibration dependences of a hue on temperature for mixtures of different compositions that characterize their temperature range and sensitivity are presented in Fig. 1. Using the developed programs of digital processing of images and the calibration dependence of a hue on temperature, one can obtain the quantitative distribution of temperature on a test surface.

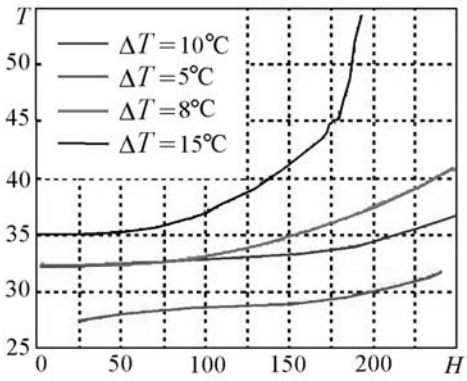

Fig. 1. Calibration dependences of hue on temperature for the CLC mixtures of different compositions with the width of the operating region ΔT = (5–15)°C. H, deg; T, °C.

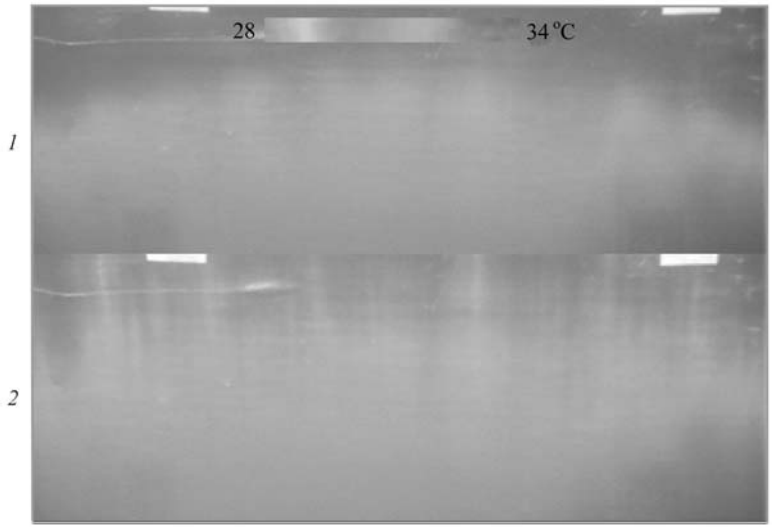

Fig. 2. LC visualization of the structure of the boundary layer on the leeward side of the wing without acoustic effect (1) and with its effect of frequency f = 500 Hz (2) with the flow directed downward, α = 5.6°, U_∞ = 10 m/s.

Below, as an illustration of the possibilities of polymeric liquid-crystal coatings and of the LCT method, we present the results of the application of this method for investigating the structure of a boundary layer and thermal heating in subsonic and hypersonic facilities.

Panoramic Visualization of the Near-Wall Flow Structure. The panoramic visualization of the near-wall flow structure at subsonic flow velocities by the LCT method, the high-temperature sensitivity of this method, and its informativeness were demonstrated, in particular, in [12–14]. In this paper, as an illustration we present the results of a parametric investigation of a separation flow on a symmetric profile. The study of separation flows and of the methods of controlling them is important for engineering applications, since such flows are extensively distributed in practice. This justifies the great amount of effort that has gone into the study of the instability and transition to turbulence in the case of separation flows [15–18].

In particular, we have investigated the phenomenon of the appearance of longitudinal structures in the region of reattachment of a boundary layer on the wing profile installed at a large angle of attack [19]. The interest in the longitudinal structures appearing in shear flows was due to their substantial role in the process of laminar–turbulent transition.

Experiments were conducted in the ITAM's subsonic low-turbulence (Tu < 0.04%) T-324 wind tunnel with dimensions of the test section 1000 × 1000 × 4000 mm. The investigations were carried out on a model of a symmet-

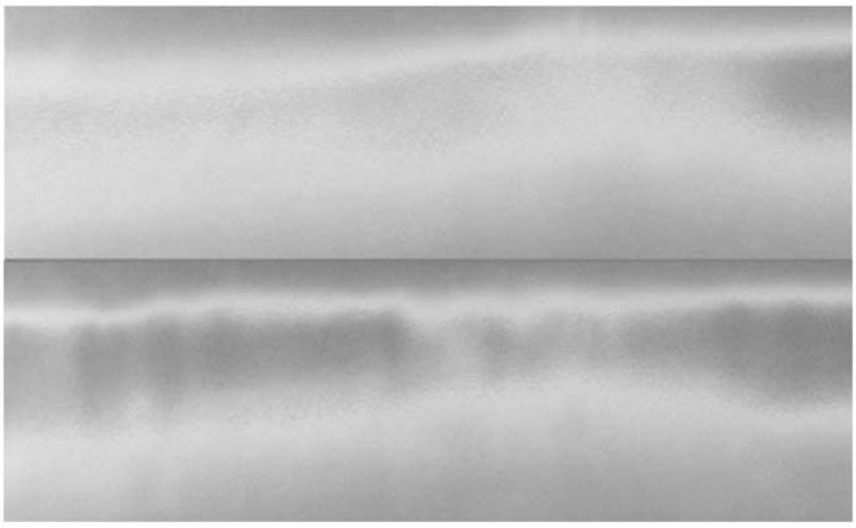

Fig. 3. Visualization of the structure of the boundary layer on the leeward side of the wing without acoustic effect (1) and with interaction at the frequency f = 2500 Hz (2) with the flow directed downward, $\alpha = 18^{o}$, U_{∞} = 10 m/s.

ric profile of a wing with a chord of 232 mm, a span of 335 mm, and a relative thickness of 15% for two angles of attack: 5.6^{o} and 18^{o}. The encircling flow velocity was 10 m/s.

Investigations were carried out in both a natural case, i.e., in the absence of controlled perturbations, and on superposition of acoustic disturbances. The latter were produced by a loudspeaker, installed downstream of the model, to which a sinusoidal signal of definite frequency and amplitude was applied.

The first series of experiments was carried out at an angle of attack of the wing of 5.6^{o} and an encircling flow velocity of 10 m/s ($\mathrm{Re} = 1.5 \cdot 10^{5}$). In this case, a laminar separation bubble of length along the chord of 50 mm appears. Behind the bubble, in the region of reattachment, a turbulent boundary layer is formed

Figure 2 presents fragments of the LC visualization of temperature distribution on the wing installed at an angle of attack of 5.6^{o} for the flow directed downward for the cases of natural and controlled acoustic disturbances (500 Hz). The LC visualization shows that in the case of natural perturbations in the region with $x > 130$ mm a system of longitudinal structures that manifest themselves in the form of longitudinal alternating bands of higher and lower temperatures appears. This region corresponds to the concluding stages of the formation of the laminar–turbulent transition and a turbulent boundary layer and to the accumulation of the disturbances shown by the curve obtained thermoanemometrically. The spatial arrangement of structures on the model surface does not change in the course of the experiment. Investigation of the spectrum of pulsations in a separated boundary layer has shown that the most unstable modes of this flow lie in the range 300–1000 Hz. On imposition of sinusoidal acoustic disturbances with frequencies lying inside the given range of instability, the flow structure changes. As compared to the natural case, the position and characteristic transverse scale of the longitudinal structures alter. The visualized region of the appearance of longitudinal structures is displaced upstream. Most likely this is due to the displacement of the flow reattachment point, since the rear boundary of the separating bubble is very sensitive to the level of external disturbances. On assignment of the frequency of disturbances above the upper limit of the instability range, the flow pattern coincides with that in the unperturbed case. It is evident that the formation of longitudinal structures in the region of reattachment of the separated boundary layer is attributed to the development of the instability waves in the mixing layer. According to the LC visualization data, the length of the wave formed in the region of reattachment of longitudinal structures in the transverse direction turns out to be approximately equal to the length of the excited instability wave.

At a large angle of attack of $\alpha = 18^{o}$, results analogous to the previous case were obtained, except for some differences, viz., to the most enhanced vibrations in the natural case corresponds a frequency region displaced, as compared to the previous case, to the region of higher frequencies from 1500 to 3000 Hz. Without the use of artificial disturbances the LC visualization of flow at an angle of attack of 18^{o} does not manifest the formation of longitudinal structures (Fig. 3). In measurements with artificial excitation a frequency of 2500 Hz was used.

The application in the given experiment of polymeric liquid-crystal coatings due to their high temperature sensitivity and the ability to demonstrate a panoramic picture of a temperature field in one experiment made it possible to reveal stationary longitudinal structures on the upper surface of a straight wing in a subsonic flow. It was shown that the structures appear behind the separating bubble in the region of flow reattachment. The excitation of such structures on exposure to acoustic effect at frequencies from the range of flow instability was demonstrated. The characteristic transverse scale of the originating longitudinal structures depends on the frequency of exciting vibrations and approximately corresponds to the length of the instability wave excited in the boundary layer.

Panoramic Visualization of Temperature and Measurement of Heat Fluxes in High-Velocity Facilities. The problems of heat protection are determined to a large extent by the state of the boundary layer on the surfaces of an aerospace vehicle. The numerical methods of solving problems with a boundary layer are still limited, and their creation and development are retarded in a number of cases by the absence of reliable experimental data that could in full measure satisfy the requirements of the validation of the models selected and of the methods of computational aerodynamics of gases. Therefore, only investigations in wind tunnels allow one to obtain experimental data for understanding this phenomenon and controlling it.

In experimental investigation of heat transfer and of a laminar–turbulent transition on the surface of aerodynamic models, the choice of a reliable method with a high spatial and temporal resolution is important. Visualization of flows occupies a particular place in the diagnostics of flows, giving an idea of the full flow picture. In the majority of cases, this is attained without introduction into the flow of any transducers or probes that disturb it. The use of modern light sources and of computer processing of an image allows one to obtain not only a qualitative picture of flow on the surface, but also the quantitative distribution of gas-dynamical parameters.

Rapidly varying conditions of an experiment in high-velocity setups make the task of visualization of the thermal field on the surface and of identification of thermal loadings much more difficult. The application of polymeric liquid-crystal coatings seems to be promising, since they can simultaneously ensure panoramic visualization and monitoring of the change in time of the mean surface-temperature level. From these data it is possible to obtain estimates of the mean levels of the densities of heat fluxes.

Under the conditions of a short-duration experiment, it is necessary to take into account the thermal inertia of film heat indicators. The thermal inertia of LC depends on the composition of the LC mixture, the geometry of LC capsules and of the measured layers and their thermophysical properties, as well as on the conditions of heat transfer on the surface, and on the direction of the thermal process (heating or cooling). The response time of an LC coating is composed of the lag time attributable to the heat conduction in the measured layer and the response time of the molecular structure of the LC. The calculated and experimental values of these parameters given in the literature are contradictory and may serve only for rough estimations. An analysis of the literature data shows that despite the fact that the time of reorientation of the pure molecules of a LC is about 3 ms [20], the time constant of the encapsulated LCs is an order of magnitude higher. In [21], the limiting value of the time constant and the upper-boundary transmission frequency were obtained theoretically, and they are equal to 1.5–45 ms and 4–500 Hz, respectively. In [22], the time constant for an LC layer of thickness 25 μm on a thin steel foil was measured experimentally and was equal to 36 ms. Based on these data, a conclusion can be drawn that at times of measurement lower than 30–40 ms mainly panoramic visualization of the flow structure can be useful, whereas measurements of heat transfer with the use of static calibration of an LC coating can be inaccurate. When an experiment lasts longer, there appears the possibility of not only visualizing the flow around a model, but also of obtaining quantitative data on the distribution of thermal loads on the model surface. The polymeric liquid-crystal coatings developed at the ITAM were tested to determine heat-flux densities under the conditions of a hypersonic flow around a model.

The LCT method was tested under the conditions in the ITAM's hypersonic installations operating periodically (AT-326) and intermittently (AT-303). The experiments were run at the Mach numbers $M \approx 6$, 11, and 14, respectively [23–25]. The AT-326 installation is a batch-operated blow-off wind tunnel with a nozzle-cut diameter of 200 mm, test-section length of 400 mm, and regime duration of up to 20 min, whereas the AT-303 installation is a short-duration, adiabatic-type wind tunnel with a nozzle cut diameter of 300–800 mm and regime duration of 0.2–0.5 s.

To find stationary heat fluxes in the AT-326 in aerodynamic experiments on models made from a heat-insulating material, the exact solution of the equation of unsteady-state heat conduction for a semi-infinite body was used under boundary conditions of the third kind, i.e., at a constant heat-transfer coefficient on the model surface.

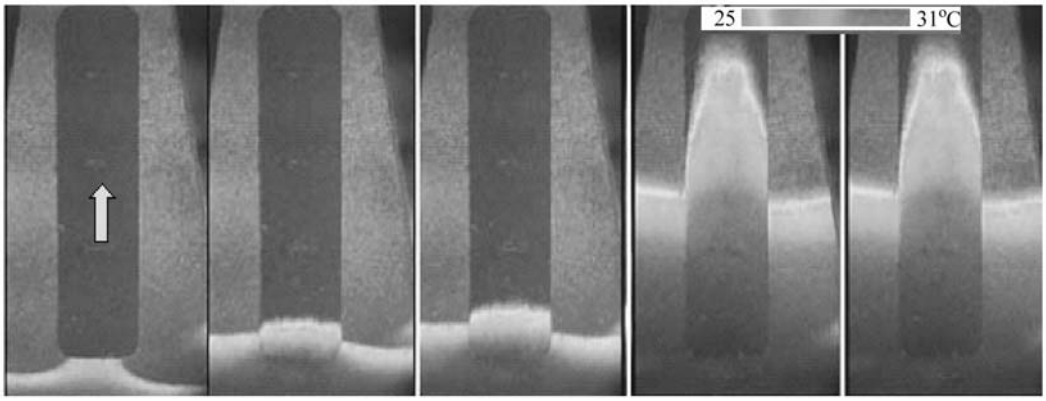

Fig. 4. Visualization of heating of a metal plate with a heat-insulated insert at M = 6.

The calculation of the heat-flux densities in the AT-303 installation was carried out using, for a model of a semi-infinite body, a nonstationary method typical of short-duration installations. To obtain estimations of the heat-flux densities on condition that $\Delta T = (T_{LC} - T_{in}) << (T_r - T_{in})$, it is permissible to use the exact solution of the heat-conduction equation at boundary conditions of the second kind, i.e., at a constant density of a heat flux to the model surface: $q(t)$ = const. It is assumed that the same boundary conditions are realized in experiments in the AT-303. The temperature increment was measured with the aid of an LC at two time instants.

On the basis of the measured temperature distributions, the dimensionless modified Stanton numbers were calculated: $\mathrm{St}_{mod}(t) = \dfrac{q(t)}{\rho_e C_p U_e (T_0(t) - T_w(t_0))}$. The heat-flux density is calculated as

$$q(t) = \frac{\sqrt{\pi \cdot \rho \cdot c \cdot \lambda} \cdot \Delta T_w(\tau)}{2\sqrt{\tau}} = \frac{\sqrt{\pi \cdot \rho \cdot c \cdot \lambda} \cdot (T_w(t) - T(t_0))}{2\sqrt{(t - t_0)}} .$$

In the AT-326 wind tunnel, the flow structure and aerodynamic heating of a flat plate at the encircling flow Mach number M = 6, stagnation pressure $P_0 \approx 10^6$ Pa, and stagnation temperature from 180 to 277°C was investigated in the range of unit Reynolds numbers based on the encircling flow parameters, $\mathrm{Re}_{1\infty} = (7.9–9.6)\cdot 10^6$. The regime lasted for about 10^{-12} s. Mounted into the plate was a changeable rectangular insert from a heat-insulating material pierced by three surface tape thermocouples. A polymeric liquid-crystal coating was applied to the plate. Wide-temperature ($\Delta T \approx$ 10–20°C) and narrow-temperature ($\Delta T \approx$ 2–6°C) temperature-indicating compositions have been developed. Measurements of the calibrating color-temperature characteristics of coatings were made with the aid of spectral and/or calorimetric analysis. After the flow regime had been attained, a homogeneously heated model was introduced into the flow with the aid of a quick lead-in mechanism. The color image of the temperature fields in the process of experiment was registered by a camera with a frame rate of 25 Hz (Fig. 4).

The experiments have shown that on a smooth plate a laminar boundary layer that is very sensitive to the encircling flow perturbations is realized. The specific feature of LC coatings is their high temperature sensitivity, which makes it possible to reveal the characteristic feature of the flow around a model. For example, in Fig. 5 vortices are seen (1) which were induced by microroughnesses localized upstream (the flow is from left to right). The influence of the difference in the thermophysical characteristics of the model is also revealed by the LC visualization (2). The influence of the longitudinal spreading of heat on a metal plate and on the thermally insulated insert distorts the form of the isotherm (3). From Fig. 5 it is also seen that the heat insulator is heated more rapidly (the isotherm is ahead) than the metal part of the surface on which lower values of the heat-transfer coefficients are realized due to the spreading and removal of heat. In the given case, the video image clearly demonstrates the influence of the boundary conditions (an adiabatic and nonadiabatic wall) on heat transfer. Even qualitative visualization of temperature fields, especially with high-temperature sensitivity, is highly informative. Visualization in real time allows a researcher to see the perturbations that appear in a boundary layer as a result of his or her manipulations and those that are attributable

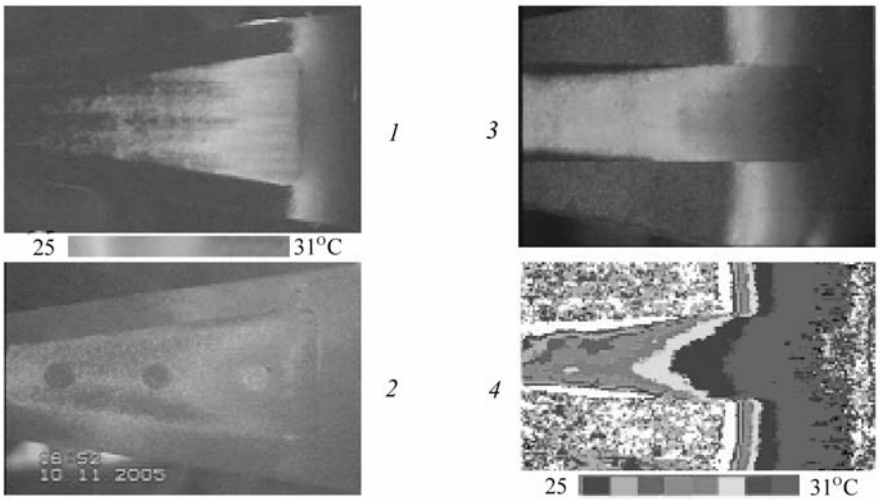

Fig. 5. LC visualization of the temperature field on the plate: 1) influence of microroughnesses on the frontal edge of the plate; 2) influence of the thermophysical characteristics of the model material; 3) influence of the longitudinal spreading of heat over the plate on the shape of the isotherm; 4) temperature field obtained from the LC data for case (3).

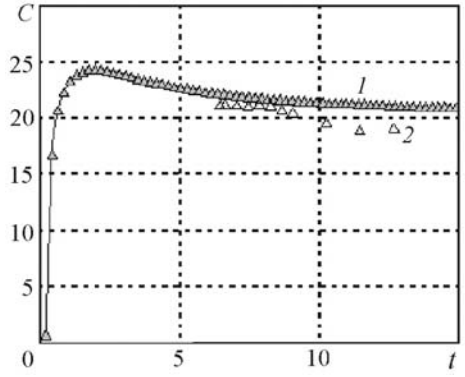

Fig. 6. A comparison of the heat-transfer coefficients obtained on the plate with the aid of film thermocouples (1) and by the LCT method (2). C, W/m^2·K; t, s.

to the flow. It allows one to select the places for setting discrete sensors and to visually control the course of the experiment, for example, the state of the model and the presence of defects on the surface, the precision of the assembly of parts, the position of the model in space, the presence of heat leaks, etc. These factors directly influence the errors of the obtained experimental data, and in the case of measuring by discrete methods they do not become evident.

Figure 6 presents for comparison data on heat fluxes in the AT-326 that were obtained with the aid of LC thermography and film sensors of heat fluxes [24]. The greatest discrepancy between the data in various runs did not exceed 15%. An analysis of errors has shown that the greatest effect on the results is exerted by the deviation from the operating conditions, in particular, the stagnation temperature T_0. For technical reasons, the instability of this parameter constituted about 10°C. This is greatly responsible for the discrepancy of the data obtained by various methods.

In the short-duration AT-30, wind tunnel3 experiments were carried out on three models manufactured from a heat-insulating material: two standard cones and a model of a returning ballistic apparatus [26–27]. The first standard model was a pointed circular cone with an apex angle of 25° and a height of 203 mm (Fig. 7). The second model was a hemisphere-blunted cone with a hemisphere radius of 20 mm (Fig. 8).

Experiments were carried out with a profiled nozzle with its outlet cross section equal to 400 mm. Preliminarily, the LCT method was tested on standard models at the encircling flow Mach number M ≈ 10.9 and the unit

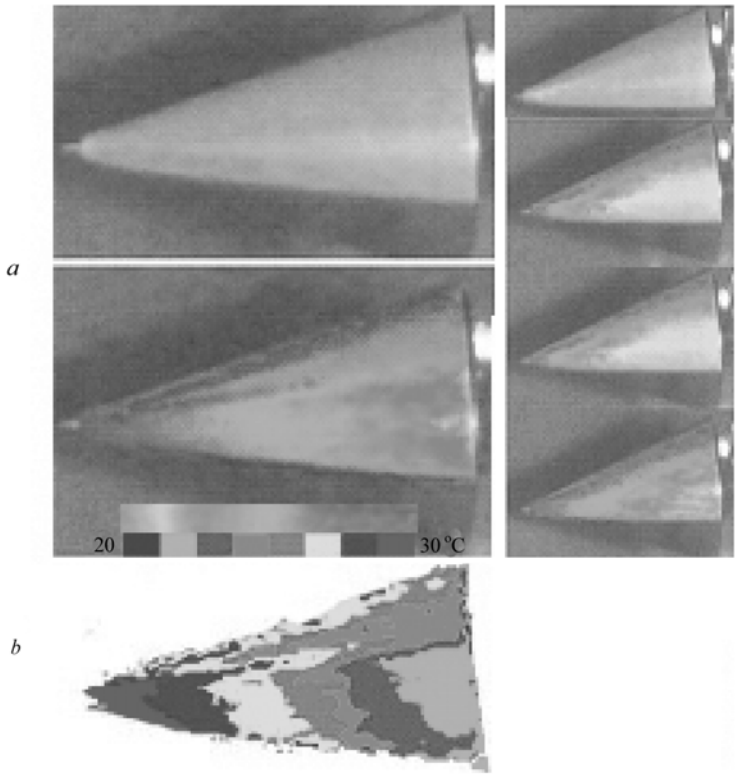

Fig. 7. LC visualization of heating (a) and the temperature chart (b) on the pointed cone obtained by the LCT method.

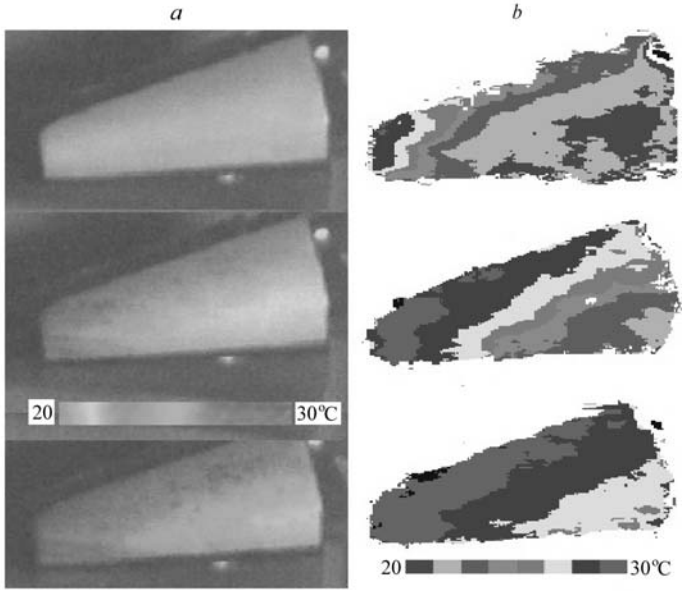

Fig. 8. LC visualization of heating (a) and the temperature chart (b) on the blunt cone obtained by the LCT method.

Reynolds number $\mathrm{Re}_1 \approx 3.0 \cdot 10^6$ m. The Reynolds number along the length of the generating line of the model was equal to $\mathrm{Re}_L \approx 0.58 \cdot 10^6$. The stagnation temperature for the time of regime existence varied within the range T_0 = 1400–1420 K and the stagnation pressure was equal to P_0 = (93–98)·10^5 Pa. The initial temperature of the model surface was close to room temperature, which ensured the value of the temperature factor $T_w/T_0 \approx 0.2$. Under the condi-

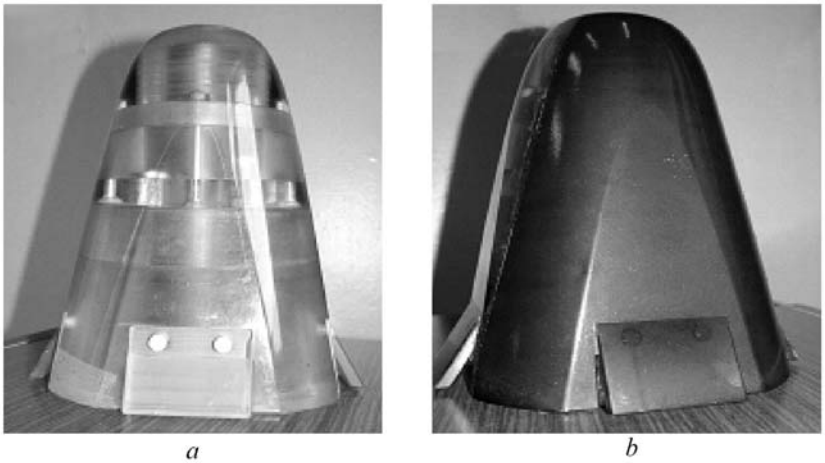

a *b*

Fig. 9. EXPERT-B model (a), model a with an LC coating (b).

tions of the AT-303 wind tunnel, the heat loading has a character close to the stepwise one — the time of the regime attainment was 5–10% of that of the experiment.

Typical pictures of the LC visualization of the change in the temperature field in the course of an experiment over the surfaces of standard models obtained by the method of liquid-crystal coatings are shown in Fig. 7 (for the pointed cone) and in Fig. 8 (for the blunt cone).

Figure 7 demonstrates the LC visualization and the temperature field, obtained from the LCT data, over the surface of the pointed cone installed at a zero angle of attack. The interval of time between the frames was 40 ms. The visualizability of the LC thermograms is due to the fact that on the assumption of the constancy of the mean level of heat fluxes to the model surface, the isocaloric (identically colored) portions of the surface correspond to the same values of specific heat fluxes. In the upper part of the cone, one can clearly see the thermal trace left by two longitudinal vortices induced by the upstream microroughness. The disturbance of the axisymmetricity of the color picture can be explained by the inaccuracy of the installation of the model at the zero angle of attack.

The third model — the model of a returning ballistic apparatus EXPERT-B — was manufactured as a one-seventh scale model relative to full-scale dimensions and had changeable nose parts (Fig. 9). The total length of the generating line was $L_1 = 221.14$ mm; the cone half-apex angle $\theta = 12.5^{\circ}$. The length of the panel was $l = 42.76$ mm and the angle of inclination of the panel to the surface was $\varphi = 20^{\circ}$. A variant of the model with increased, as against the initial variant, transverse dimensions of the nose part, which made it possible to arrange a backward-facing step at the juncture of the nose part with the body (circular ledge), was investigated. The thermal field of the model was investigated in the same wind tunnel at the encircling flow Mach number M = 13.93 and the unit Reynolds number $\mathrm{Re}_1 = (2.36–2.43)\cdot 10^7$. The Reynolds number along the length of the projection of the model generating line $L = 0.2214$ m on the x axis was $\mathrm{Re}_L \approx 5.42\cdot 10^6$. The stagnation temperature for the time of regime existence varied in the range $T_0 = 1260–1300$ K, the stagnation pressure was equal to $P_0 \approx 10^8$ MPa, $T_w/T_0 \approx 0.23$. The duration of the operating conditions varied from 40 to 350 ms. For simultaneous visualization over the entire portion of the surface, the composition of a liquid-crystal mixture was selected in conformity with the temperature change expected on it $\Delta T(x, y, t)$. In the experiments considered, LC coatings were used which had a width of the region of selective reflection equal to $\Delta T \approx 10–20^{\circ}$C. With a maximum temperature working range of the LC indicator of 20°C and duration of the operating conditions of 40 ms, the indicator made it possible to measure the heat-flux density not higher than $q_{\max} \approx 0.05$ MW/m^2.

One of the tasks of the investigations carried out was visualization of the influence of the height of the circular ledge located at the place of juncture of the nose and conical parts of the model on the temperature field. Figure 10 presents the LC visualization of temperature distribution on the conical parts of the models with ledges of different heights: $h = 0$, 1, and 2 mm. The presence of the ledge leads to the formation of a separation zone downstream of the ledge with subsequent flow reattachment. In both cases $h = 1$ and 2 mm, in the region behind the ledge there occurs a relative lowering of temperature. As the height of the ledge increases, the line of flow attachment downstream

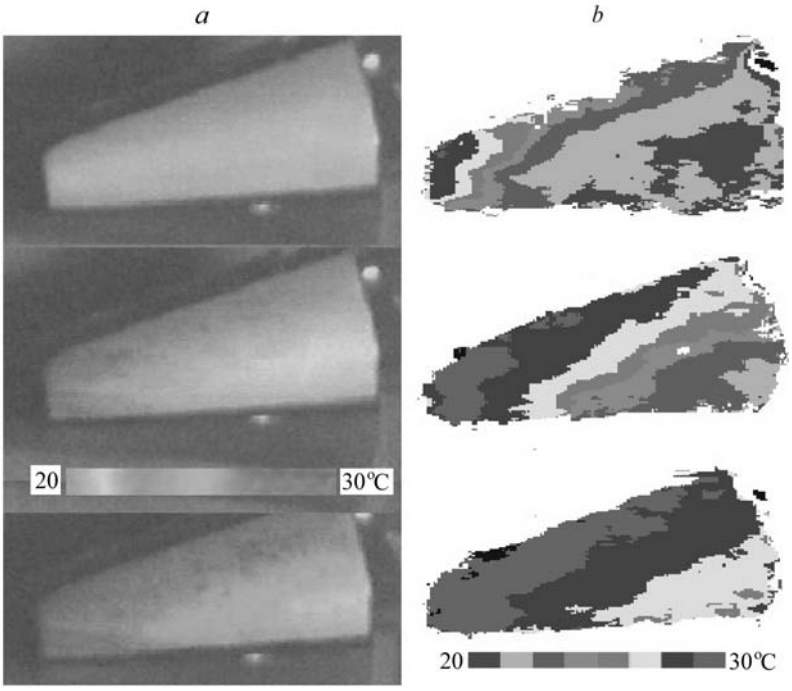

Fig. 10. LC visualization of temperature field on models with ledges at t = 40 ms and $\gamma = 45^{o}$: 1) h = 0; 2) 1; 3) 2 mm.

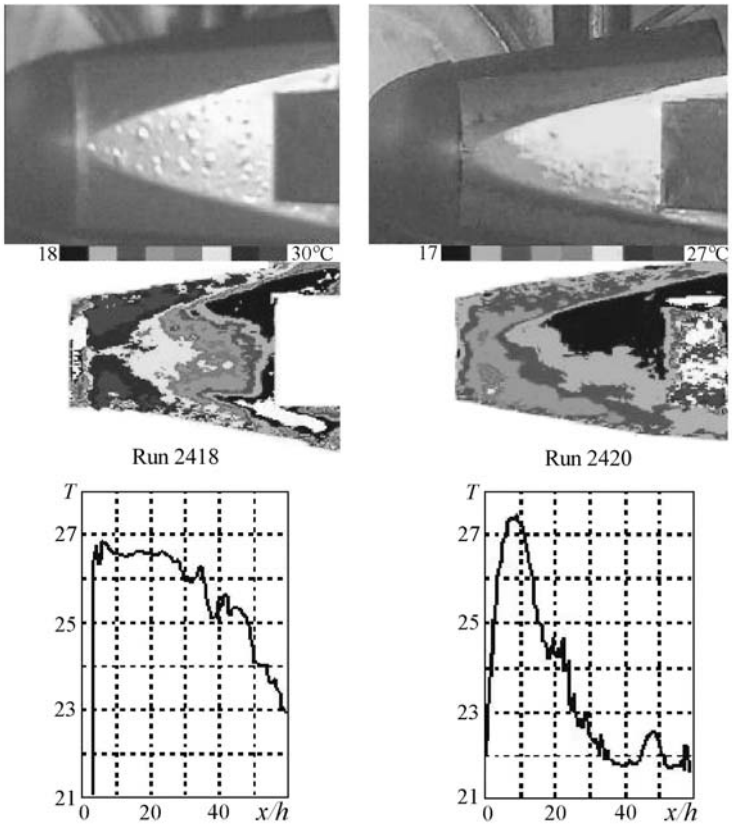

Fig. 11. LC visualization (from above), chart of temperatures and graphs of temperature change along the longitudinal axis of the model from the ledge to the panel for h = 2 mm at t = 40 ms. T, ^{o}C.

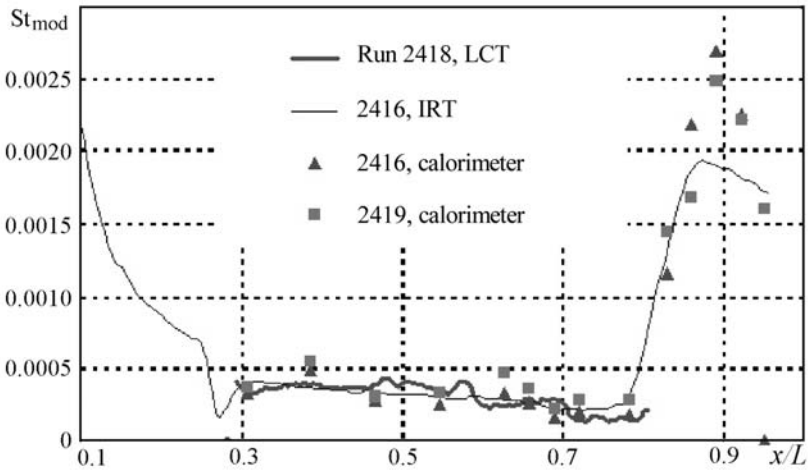

Fig. 12. A comparison of the modified Stanton numbers obtained by three methods at t = 40 ms.

of the ledge on the conical portion of the surface of the model decreases downstream. The relative decrease in the temperature of a subsonic flow in the recirculation zone downstream of the ledge is accompanied by a small increase in the thermal load level in the reattachment zone.

Figure 11 presents the temperature charts and graphs of the change in temperature along the model surface with a circular ledge of height h = 2 mm over the portion with the panel in two runs 2418 and 2420. In the run 2420 the picture of temperature distributions turned out to be nonsymmetric, with the result that the graphs of the temperature change differ noticeably. The obtained asymmetry is explained by the inaccurate installation of the model at the angle of attack (not more than 0.5°C). The change of the temperature field points to the sensitivity of the thermal process to flow regime and simultaneously to the sensitivity of the visualization method applied.

The authenticity of the results obtained is confirmed by the good convergence of the data of the LCT for the main part of the EXPERT model body with the results obtained by other research workers at the ITAM on this model, viz., by the panoramic method of infrared thermography (IRT) and the discrete calorimetric method [28, 29]. For discrete measurement of the heat fluxes, the models were pierced by calorimetric transducers of thermocouple type. The standard error of determining a heat flux by calorimetric transducers which includes the errors of reproduction of the encircling flow parameters in the AT-303 did not exceed 10%. The panoramic distribution of the temperature field changed with the aid of a fast thermographic complex based on the SVIT-type infrared imager developed and manufactured at the Institute of Semiconductor Physics of the Siberian Branch of the Russian Academy of Sciences. The temperature resolution of the thermographic complex was 0.027°C, the temporal resolution was 0.010 s. Figure 12 presents a comparison of the modified Stanton numbers at close instants of time on the conical part of the model (downstream of the ledge with h = 2 mm) obtained by these three methods.

Conclusions. The unique optical properties of liquid crystals, namely, their high sensitivity to external effects, finds application in the development, based on them, of new heat-sensitive materials for panoramic diagnostics of surface temperature fields in aerophysical experiments. At the present time, due to the application of computers, the use of such materials is possible not only for the visualization of temperature fields, but also for measuring them. The charts of temperature distributions obtained on their basis allow experimentalists to investigate in detail the flow structure near the surface and develop methods of monitoring this structure. The approaches developed are applicable for a wide range of problems of investigation of the fine structure of wall flows and heat transfer.

NOTATION

C, heat-transfer coefficient, W/(m^2·K); c, specific heat, J/(kg·K); C_p, specific heat of air, J/(kg·K); f, frequency of acoustic action, Hz; h, ledge height, m; l, length of the panel; L, model length, m; M, Mach number; P_0, stagnation pressure, Pa; q, heat-flux density, W/m^2; Re_1, Reynolds number based on the characteristic dimension of 1

m; St_{mod}, modified Stanton number; t_0, initial time, s; Δt, time integral, s; T_0, stagnation temperature of a flow, K; T_w, surface temperature of a model, K; T_r, recovery temperature; T_{LC}, current temperature of the LC coating, K; T_{in}, initial temperature of the model, K; $Tu = \sqrt{u'^2}/U_\infty$, degree of flow turbulence, %; u', fluctuations of the longitudinal flow-velocity component, m/s; U_∞, encircling flow velocity at infinity, m/s; U_e, encircling flow velocity, m/s; x, y, longitudinal and transverse coordinates; α, angle of attack assigned in the vertical plane of the tunnel, deg; $\varepsilon = (\rho c \lambda)^{0.5}$, coefficient of thermal activity, $W \cdot m^2 \cdot K^{-1} \cdot s^{-0.5}$; θ, half-apex angle of the cone, deg; λ, thermal conductivity, J/(s·m·K); ρ, density, kg/m^3; ρ_e, encircling flow density, kg/m^3; τ, time, s; φ, angle of panel inclination, deg. Subscripts: e, encircling flow; r, recovery; w, wall.

REFERENCES

1. E. J. Klein, Liquid crystals in aerodynamic testing, *Astronautics and Aeronautics*, No. 6, 70–73 (1968).
2. G. M. Zharkova, Visualization of temperature fields by method of LC, *Exp. Heat Transfer*, No. 4, 85–94 (1991).
3. T. Jones, Liquid crystals in aerodynamic and heat transfer testing, *Proc. Int. Seminar on Optical Methods and Data Processing in Heat and Fluid Flow*, London (1992), pp. 51–66.
4. G. M. Zharkova, V. N. Kovrizhina, V. I. Kornilov, and A. A. Pavlov, Registration of temperature fields with the aid of liquid-crystal coatings, *Teplofiz. Aéromekh.*, **3**, No. 4, 317–324 (1996).
5. P. G. de Gennes, *The Physics of Liquid Crystals* [Russian translation], Mir, Moscow (1977).
6. A. S. Sonin, *Introduction to the Physics of Liquid Crystals* [in Russian], Nauka, Moscow (1983).
7. V. F. Belyakov and A. S. Sonin, *The Optics of Cholesteric Liquid Crystals* [in Russian], Nauka, Moscow (1982).
8. G. M. Zharkova and A. S. Sonin, *Liquid Crystal Composites* [in Russian], Nauka, Novosibirsk (1994).
9. G. M. Zharkova, V. N. Kovrizhina, and V. M. Khachaturyan, Experimental investigation of subsonic flows by the method of liquid-crystal tomography, *Prikl. Mekh. Tekh. Fiz.*, **43**, No. 2, 122–128 (2002).
10. G. M. Zharkova, V. N. Kovrizhina, and V. M. Khachaturyan, Calorimetric analysis in the liquid-crystal tomography, in: *Proc. 6th Int. Sci.-Tech. Conf. "Optical Methods of Studying Flows"* (OMSF 2001), 26–29 June 2001, Moscow (2001), pp. 114–117.
11. G. M. Zharkova and V. N. Kovrizhina, Application of liquid crystals for investigating heat transfer and flow structure in a channel with corrugated walls, *Teplofiz. Aéromekh.*, **9**, No. 1, 103–111 (2002).
12. A. V. Dovgal, G. M. Zharkova, B. Yu. Zanin, and V. N. Kovrizhina, A liquid crystal coatings application for flow separation investigation, *Sci. Ann. TsAGi*, **32**, No. 3/4, 157–163 (2001).
13. A. P. Brylyakov, G. M. Zharkova, B. Yu. Zanin, V. N. Kovrizhina, and D. S. Sboev, Flow separation on a straight wing under increased external turbulence, *Uch. Zap. TsAGI*, **35**, Nos. 1–2, pp. 57–62 (2004).
14. G. M. Zharkova, B. Yu. Zanin, V. N. Kovrizhina, and A. P. Brylyakov, Free stream turbulence effect on the flow structure over the finite span straight wing, *J. Visualization. Japan*, **5**, No. 2, 169–176 (2002).
15. J. H. Watmuff, Evolution of a wave packet into vortex loops in a laminar separation bubble, *J. Fluid Mech.*, **397**, 119 (1999).
16. C. P. Häggmark, A. A. Bakchinov, and P. H. Alfredsson, Experiments on a two-dimensional laminar separation bubble, *Phil. Trans. R. Soc. Lond.*, **A 358**, 3193 (2000).
17. V. N. Brazhko, Some features of cross flow periodicity in two-dimensional supersonic separated regions, *Sci. Ann. TsAGi*, **22**, No. 4, 25 (1991).
18. V. I. Kornilov, *Three-Dimensional Turbulent Near-Wall Flows in Streamwise Corners*, Nauka, Siberian Publishing Firm of RAS, Novosibirsk (2000).
19. A. P. Brylyakov, B. Yu. Zanin, V. N. Kovrizhina, and G. M. Zharkova, Acoustic excitation of stationary streamwise structures in a separation region on a straight wing, *Phys. Fluids*, **17**, No. 7, pp. 078107–078111 (2005).

20. P. T. Ireland and T. V. Jones, The response time of a surface thermometer employing encapsulated thermochromic liquid crystals, *J. Physics E: Sci. Instrum.*, **20**, 1195–1199 (1987).
21. R. Lemberg, *Liquid Crystal for the Visualization of Unsteady Boundary Layers: M. S. Thesis*, Illinois Institute of Technology (1970).
22. R. Parker, Transient surface temperature response of liquid crystal films, *Laurence Livermore Lab.*, Rept. UCLR-73583 (1971).
23. G. M. Zharkova, V. N. Kovrizhina, A. P. Petrov, B. V. Smorodsky, H. Knauss, T. Roediger, S. Wagner, and E. Kraemer, Comparative heat transfer studies at hypersonic conditions by means of three measurement techniques. Part I: Measurement techniques, experimental setup and preceding investigations, *Proc. XIII Int. Conf. on the Methods of Aerophysical Research* (ICMAR 2007), Novosibirsk, Russia, pp. 221–228.
24. G. M. Zharkova, V. N. Kovrizhina, A. P. Petrov, B. V. Smorodsky, H. Knauss, T. Roediger, S. Wagner, and E. Kraemer, Comparative heat transfer studies at hypersonic conditions by means of three measurement techniques. Part II: Comparison of measurements with theoretical estimations, *Proc. XIII Int. Conf. on the Methods of Aerophysical Research* (ICMAR 2007), Novosibirsk, Russia, pp. 229–235.
25. G. M. Zharkova, V. N. Kovrizhina, and A. P. Petrov, The quantitative temperature visualization for heat transfer study under hypersonic velocities, *12th Int. Symp. on Flow Visualization*, 10–14 September 2006, German Aerospace Center (DLR), Göttingen, Germany (2006).
26. V. N. Kovrizhina, A. M. Kharitonov, A. P. Petrov, S. I. Schpack, G. M. Zharkova, and V. I. Zvegintsev, The study of hypersonic heat transfer by liquid crystals thermography, *Proc. 6th European Symp. on Aerothermodynamics for Space Vechicles*, EUCASS, 3–6 November 2008, Versailles, France (2008).
27. G. M. Zharkova, V. N. Kovrizhina, and A. P. Petrov, Visualization and measurements by liquid crystal thermography in short-duration facility, *Proc. XIV ICMAR*, 30 June–6 July, 2008, Novosibirsk, Russia, ISBN 978-5-98901-040-0.
28. A. M. Kharitonov, N. P. Adamov, M. D. Brodetsky, L. G. Vasenyov, I. I. Mazhul, V. I. Zvegintsev, J. C. Paulat, J. M. Muylaert, and W. Kordulla, Investigation of aerogasdynamics of re-entry vehicles in the new hypersonic wind tunnel at ITAM, *Proc. 44th AIAA Aerospace Sciences Meeting and Exhibit*, 9–12 January 2006, Reno, Nevada, USA (AIAA Paper No. 2006-0499).
29. N. P. Adamov, V. F. Chirkashenko, A. M. Kharitonov, I. I. Mazhul, A. N. Shiplyuk, S. I. Shpack, V. I. Zvegintsev, and J. M. Maylaert, Aerothermodynamics of EXPERT ballistic vehicle at hypersonic speeds, *European Conf. for Aerospace Sciences*, EUCASS, 6–9 July 2009, Versailles Conference Center, Paris, France (2009).